

A New 0.4-V 27-dB 3.1-10.6-GHz UWB Low-Noise Amplifier with Dual-Band B and pass Filter

To-Po Wang, Jai-Yang Syu

Abstract—A low-voltage high-gain ultra-wideband (UWB) low-noise amplifier (LNA) with dual-band tunable bandpass filter for interference rejection is proposed in this paper. There are two sections of the proposed multi-band tunable bandpass filter. The first one is designed for 2.4-GHz interference rejection, and the other one is for 5.2-GHz interference blocking. In addition, high- Q active inductors are adopted in each bandpass filter section for improving the interferences rejection. According to the proposed circuit topology, the UWB LNA has been designed in 0.18- μm CMOS process. Simulated results confirm the UWB LNA combining the proposed dual-band tunable bandpass filter can effectively achieve high gain of 27 dB, low noise figure of 2.8 dB, low LNA supply voltage of 0.4 V, and total dc power consumption including multi-band tunable bandpass filter of 16.4 mW. In addition, the simulated interference rejections at 2.4 GHz and 5.2 GHz are 46 dB and 29 dB, respectively.

Index Terms—interference rejection, low-noise amplifier (LNA), noise figure, notch filter.

I. INTRODUCTION

Because of the blossom of high-speed high-data-rate transmission, the requirements of radio-frequency integrated circuits are increased. For UWB applications, one of the critical function blocks is LNA design [1]-[8]. In [1], a UWB LNA with low dc power consumption for 3.2 to 9.7 GHz is presented. A high interference rejection at stop band designed in a 0.18- μm CMOS process. Two notch filters are adopted, the first one is the passive band-pass filter for 1.1-GHz, 15-GHz, and 27.6-GHz interferences rejection, and the other one is the active notch filter for 2.4-GHz interference rejection. Therefore, several stop-band interference rejections are created at 0.9 GHz, 1.8 GHz, and 2.4 GHz are 53.3 dB, 26.4 dB, and 26.5 dB.

To increase the operation bandwidth and provide a flat small signal gain (S_{21}), the RC shunt-shunt feedback is utilized [2]. Moreover, a parallel RLC load is deposited at the output terminal. Based on these methods, a broadband S_{11} is achieved. The UWB LNA in [2] exhibits the maximum gain of 13.33 dB, minimum noise figure of 2.68 dB, supply voltage of 1.8 V, and dc power consumption of 11.8 mW. In [3], wideband LNAs using parallel-to-series resonant matching network between common-gate and common-source stages are presented. The LNA consists of two stages, the first stage is the common-gate stage, and the second stage is the common-source stage.

By utilizing interstage-matching technology, the UWB LNA achieves the maximum gain of 12.7 dB, minimum noise figure of 2.5 dB, supply voltage of 0.7 V at first stage, 1.5 V at second stage, and dc power consumption of 13.4 mW. In [5], a dual-channel shunt technique is adopted to a CMOS LNA. One channel uses inductive-series peaking for improving the gain flatten, and the other one adopts resistive feedback to realize the wideband input matching network. Based on these techniques, the 0.18- μm CMOS UWB LNA achieves a maximum gain of 10.2 dB with input return loss (S_{11}) better than 9 dB over a 3-dB bandwidth from 0.5 to 11 GHz. The dc power consumption is 14.4 mW, and the measured noise figure is from 3.9 to 4.5 dB. To lock interferences, a low-noise amplifier with tunable interference rejection is presented [6]. A tunable active notch filter is embedded to a 3.1-10.6-GHz UWB LNA, leading to an improved interference rejection. The LNA exhibits the maximum power gain of 13.2 dB and the lowest noise figure of 4.5 dB. In addition, the interference rejection is 8.2 dB and the dc current is 12.8 mA from 1.8-V supply voltage.

In this work, a dual-band bandpass filter is proposed. The bandpass filter includes high- Q active inductors and varactors. According to the simulated results, the proposed UWB LNA using the proposed bandpass filter achieves the good interference rejections at 2.4 and 5.2 GHz.

II. PROPOSED UWB LNA

Fig. 1 illustrates the circuit schematic of the proposed 3.1-10.6-GHz UWB LNA. To exhibit low-voltage and high gain, three common-source stages are cascaded, leading to a 0.4-V supply voltage and 27-dB power gain. Moreover, the common-source topology serves as the first stage for achieving a low noise figure of 2.8 dB. In order to block the interference signals, a high-rejection dual-band bandpass filter is proposed to integrate with the UWB LNA, as shown in Fig. 1. The notch filter is deposited between the LNA's third stages for lowering the noise figure. According to Friis equation

$$NF_{tot} = NF_1 + \frac{NF_2 - 1}{A_{P1}} + \dots + \frac{NF_m - 1}{A_{P1} \dots A_{P(m-1)}} \quad (1)$$

Manuscript received March, 2014.

To-Po Wang, Department of Electronic Engineering and Graduate Institute of Computer and Communication Engineering, National Taipei University of Technology, Taipei, Taiwan.

Jai-Yang Syu, Department of Electronic Engineering and Graduate Institute of Computer and Communication Engineering, National Taipei University of Technology, Taipei, Taiwan.

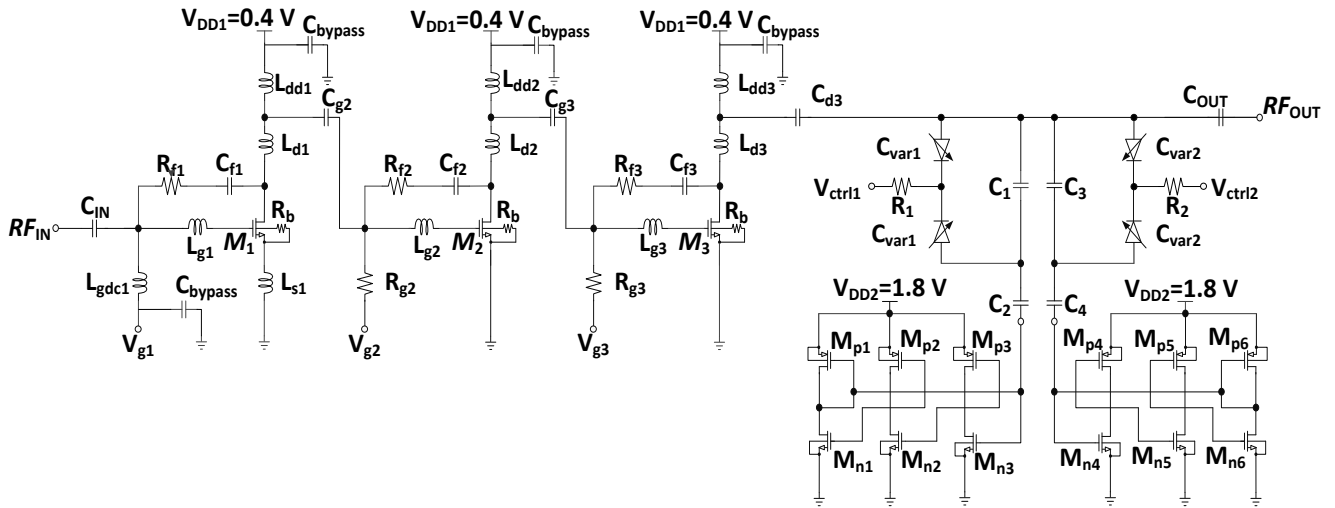


Fig. 1. Schematic of the UWB LNA with the proposed dual-band bandpass filter.

where $NF_{x, x=1...m}$ is the noise figure of each stage, $A_{p, x=1...m-1}$ is the gain of corresponding stage, and the NF_{tot} is the total noise figure, the noise performance is directly dominated by the first stage, and the noise figure of the following stages can be minimized by increasing the gain of previous stages [9]. Therefore, the dual-band bandpass filter is connected at the last stage to minimize the noise figure.

Fig. 2 depicts the proposed high-rejection dual-band tunable bandpass filter. It includes two sections, the first section is designed for 5.2-GHz interference rejection, and the second section is designed for 2.4-GHz interference blocking. In addition, each bandpass filter section comprises a high- Q active inductor and varactors for interference rejection and center frequency tuning. Fig. 3 shows the simulated transmission coefficient (S_{21}) of the proposed dual-band tunable bandpass filter. From Fig. 3, it is observed that the insertion loss at 2.7 GHz is 0.5 dB. In addition, the generated minimum S_{21} are -29.2 dB at 2.4 GHz and -24.2 dB at 5.2 GHz.

III. SIMULATION RESULTS

The proposed low-voltage low-noise high-gain UWB LNA with dual-band tunable bandpass filter has been designed in 0.18- μm RF CMOS process. Fig. 4 shows the chip layout of the proposed UWB LNA. The chip size is 1.17 x 0.9 mm^2 including the testing pads. The supply voltage of this UWB LNA is 0.4 V. The total dc power consumption of the proposed UWB LNA including the multi-band tunable notch filter is 16.4 mW. The simulation is performed by using circuit simulator Agilent's Advanced Design System (ADS) software. In addition, the inductors, capacitors, and interconnections are considered by adopting full-wave electronic-magnetic (EM) simulation tools, Sonnet and HFSS.

Fig. 5 shows the simulated S parameters of the proposed UWB LNA. From this figure, it is observed that the maximum gain of S_{21} is 27 dB. Moreover, the input/output reflection coefficients (S_{11} and S_{22}) are below -10 dB for 3.1-10.6-GHz UWB bandwidth, performing the well matched input/output circuits. Fig. 6 shows the simulated interference rejection of the proposed UWB LNA. From this figure, it is observed that the interference rejections are 46 dB at 2.4 GHz and 29 dB at 5.2 GHz. Fig. 7 shows the simulated noise figure of the proposed 3.1-10.6-GHz UWB LNA. It is indicated that the

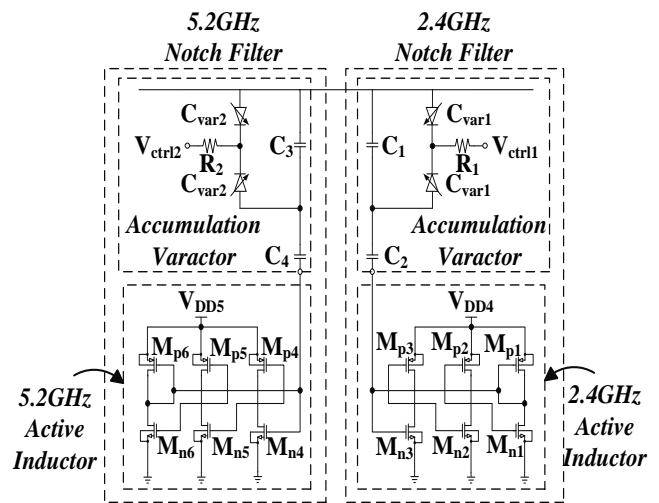


Fig. 2. Schematic of the proposed dual-band bandpass filter.

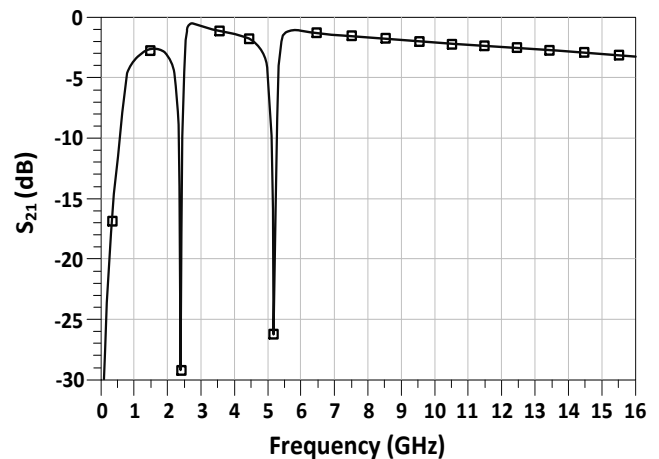


Fig. 3. Simulated transmission coefficient (S_{21}) of the proposed dual-band tunable bandpass filter.

minimum noise figure is 2.8 dB at 7.5 GHz. To consider the linearity of the UWB LNA, the simulated input-referred third-order intercept point (IIP_3) of the proposed UWB LNA is shown in Fig. 8. The two-tone test is carried out at 8 GHz, and the frequency spacing is 1 MHz. It is indicated that the IIP_3 for the proposed UWB LNA is -20 dBm.

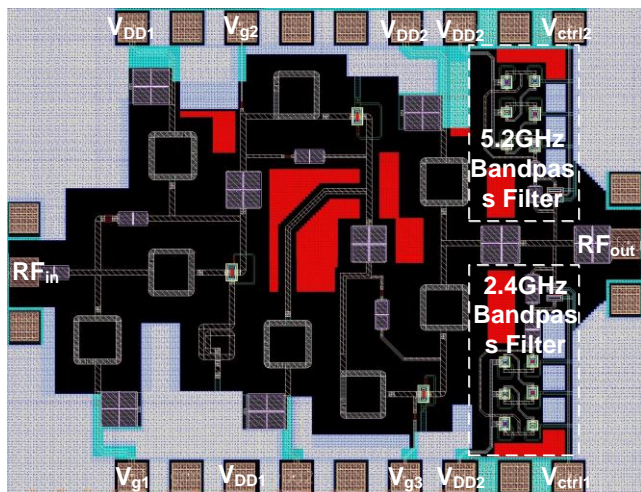


Fig. 4. Chip layout of the proposed UWB LNA with the proposed dual-band tunable bandpass filter (the overall chip size is $1.17 \times 0.9 \text{ mm}^2$).

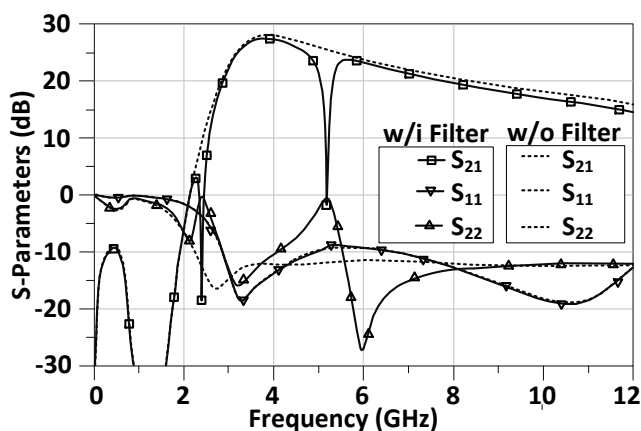


Fig. 5. Simulated S parameters of the proposed UWB LNA.

IV. CONCLUSION

The 3.1-10.6-GHz UWB LNA with dual-band bandpass filter for interference rejection is presented in this paper. Based on the proposed circuit topology, the UWB LNA can deliver high gain of 27 dB, low noise figure of 2.8 dB, low LNA supply voltage of 0.4 V, and total dc power consumption including multi-band tunable notch filter is 16.4 mW. Moreover, the simulated interference rejection at 2.4 GHz and 5.2 GHz are 46 and 29 dB, respectively. Compared to the previous published LNA with notch filter, the proposed circuit topology in this work exhibits superior performance in terms of supply voltage, noise figure, gain, and interference rejection.

ACKNOWLEDGMENT

This work is supported in part by the National Science Council of Taiwan, R.O.C., under Contract NSC 101-2119-M-027-003, NSC 102-2623-E-027-004-NU, NSC 102-2119-M-027-002, and NSC 103-2623-E-027-001-NU. The authors would like to thank the National Chip Implementation Center (CIC), Hsinchu, Taiwan, and National Nano Device Laboratories (NDL), Hsinchu, Taiwan, for technical supports.

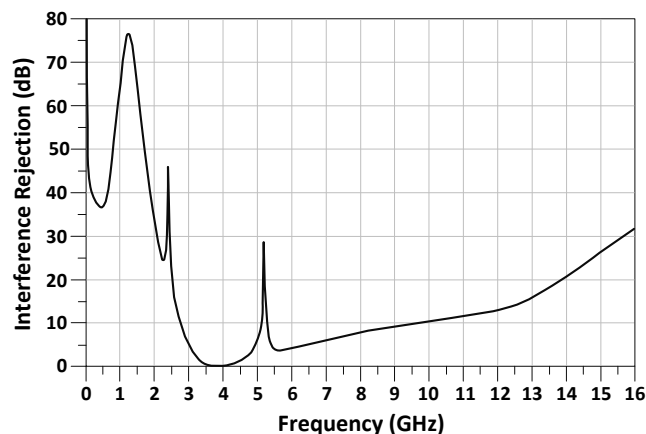


Fig. 6. Simulated interference rejection of the proposed UWB LNA.

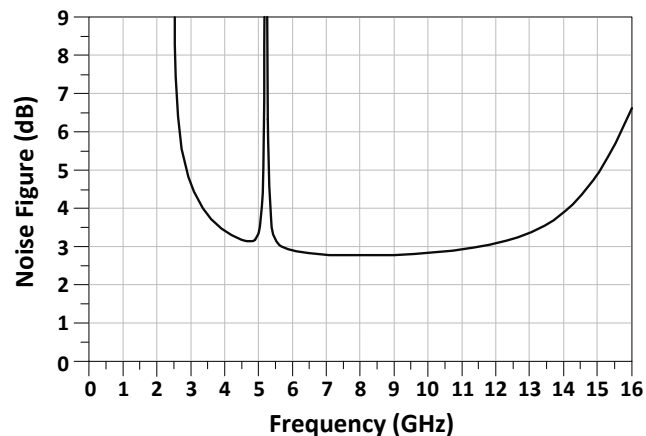


Fig. 7. Simulated noise figure of the proposed UWB LNA.

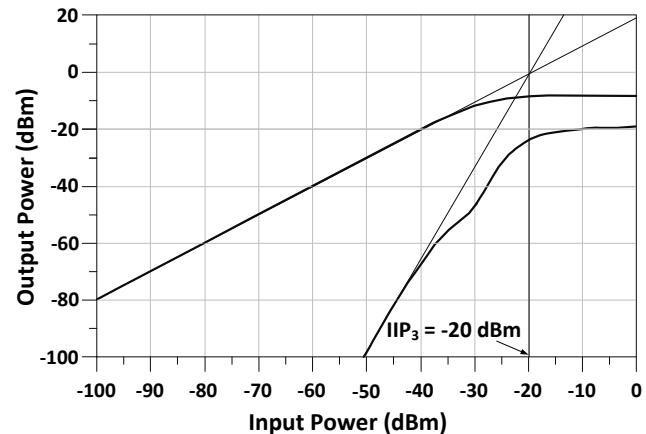


Fig. 8. Simulated input-referred third-order intercept point (IIP_3) of the proposed UWB LNA.

REFERENCES

- [1] J. F. Chang, Y. S. Lin, J. H. Lee, and C. C. Wang, "A low-power 3.2~9.7GHz ultra-wideband low noise amplifier with excellent stop-band rejection using 0.18 μm CMOS technology," in *Radio and Wireless Symp. (RWS)*, 2012, pp. 199-202.
- [2] C. H. Wu, Y. S. Lin, J. H. Lee, and C. C. Wang, "A 2.87 \pm 0.19dB NF 3.1~10.6GHz ultra-wideband low-noise amplifier using 0.18 μm CMOS technology," in *Radio and Wireless Symp. (RWS)*, 2012, pp. 227-230.
- [3] Y. T. Lo and J. F. Kiang, "Design of wideband LNAs using parallel-to-series resonant matching network between common-gate and common-source stages," *IEEE Trans. Microw. Theory Tech.*, vol. 59, no. 9, pp. 2285-2294, Sept. 2011.
- [4] J. Y. Lin and H. K. Chiou, "Power-constrained third-order active notch

- filter applied in IR-LNA for UWB standards,” *IEEE Trans. Circuits Syst. II, Express Briefs*, vol. 58, no. 1, pp. 11-15, Jan. 2011.
- [5] Q. T. Lai and J. F. Mao, “A 0.5-11 GHz CMOS low noise amplifier using dual-channel shunt technique,” *IEEE Microw. Wireless Compon. Lett.*, vol. 20, no. 5, pp. 280-282, May. 2010.
- [6] B. Park, S. Choi, and S. Hong, “A low-noise amplifier with tunable interference rejection for 3.1- to 10.6-GHz UWB systems,” *IEEE Microw. Wireless Compon. Lett.*, vol. 20, no. 1, pp. 40-42, Jan. 2010.
- [7] Y. Gao, Y. J. Zheng, and B. L. Ooi, “0.18 μm CMOS dual-band UWB LNA with interference rejection,” *Electronics Letters*, vol. 43, no. 20, pp. 40-42, Sept. 2007.
- [8] T. P. Wang and S. H. Chiang, “A 3.1-10.6 GHz ultra-wideband 0.18- μm CMOS low-noise amplifier with micromachined inductors” in *2011 IEEE International Conference on Electron Devices and Solid-State Circuits (IEEE EDSSC)*, 2011, pp. 1-2.
- [9] T. P. Wang, Z. W. Li, and H. Y. Tsai, “Performance Improvement of 0.18- μm CMOS microwave amplifier using micromachined suspended inductors: theory and experiment,” *IEEE Transactions on Electron Devices*, vol. 60, no. 5, pp. 1738-1744, May 2013.